Carcinogenesis, 2015, Vol. 36, No. 7, 792–799

doi:10.1093/carcin/bgv056
Advance Access publication April 26, 2015
Original Manuscript

ORIGINAL MANUSCRIPT

A novel role for an RCAN3-derived peptide as a tumor suppressor in breast cancer

Sergio Martínez-Høyer[1,7], Sònia Solé-Sánchez[1], Fernando Aguado[2], Sara Martínez-Martínez[3], Eva Serrano-Candelas[1,8], José Luis Hernández[4], Mar Iglesias[5], Juan Miguel Redondo[3], Oriol Casanovas[6], Ramon Messeguer[4,†] and Mercè Pérez-Riba[1,*,†]

[1]Cellular Signaling Unit, Human Molecular Genetics Group, Bellvitge Biomedical Research Institute – IDIBELL. L'Hospitalet de Llobregat 08908 Barcelona, Spain, [2]Department of Cell Biology, University of Barcelona, Barcelona, Spain, [3]Departamento de Biología Vascular e Inflamación, Centro Nacional de Investigaciones Cardiovasculares, 28029 Madrid, Spain, [4]Biomed Division, LEITAT Technological Center, Parc Cientific de Barcelona, Edifici Hèlix, 08028 Barcelona, Spain, [5]Department of Pathology, Hospital del Mar (Institut Hospital del Mar d'Investigacions Mèdiques), Autonomous University of Barcelona 08004, Barcelona, Spain, [6]Tumor Angiogenesis Group, Translational Research Laboratory, Catalan Institute of Oncology - Bellvitge Biomedical Research Institute – IDIBELL. L'Hospitalet de Llobregat 08908 Barcelona, Spain

[7]Present address: Genome Sciences Centre, BC Cancer Agency, 675W 10th Ave Vancouver, V5Z 1L3 British Columbia, Canada

[8]Present address: Biochemistry Unit, Department of Physiological Sciences I, Faculty of Medicine, University of Barcelona, Casanova 143 08036, Barcelona, Spain

*To whom correspondence should be addressed. Tel: +34 932607427; Fax: +34 932607414. Email: mpr@idibell.cat

†These authors contributed equally to this work.

Abstract

The members of the human regulators of calcineurin (RCAN) protein family are endogenous regulators of the calcineurin (CN)-cytosolic nuclear factor of activated T-cells (NFATc) pathway activation. This function is explained by the presence of a highly conserved calcipressin inhibitor of calcineurin (CIC) motif in RCAN proteins, which has been shown to compete with NFATc for the binding to CN and therefore are able to inhibit NFATc dephosphorylation and activation by CN. Very recently, emerging roles for NFATc proteins in transformation, tumor angiogenesis and metastasis have been described in different cancer cell types. In this work, we report that the overexpression of RCAN3 dramatically inhibits tumor growth and tumor angiogenesis in an orthotopic human breast cancer model. We suggest that RCAN3 exerts these effects in a CN-dependent manner, as mutation of the CIC motif in RCAN3 abolishes the tumor suppressor effect. Moreover, the expression of the EGFP-R3$^{178-210}$ peptide, spanning the CIC motif of RCAN3, is able to reproduce all the antitumor effects of RCAN3 full-length protein. Finally, we show that RCAN3 and the EGFP-R3$^{178-210}$ peptide inhibit the CN-NFATc signaling pathway and the induction of the NFATc-dependent gene cyclooxygenase-2. Our work suggests that the EGFP-R3$^{178-210}$ peptide possess potent tumor suppressor properties and therefore constitutes a novel lead for the development of potent and specific antitumoral agents. Moreover, we propose the targeting of the CN-NFATc pathway in the tumor cells constitutes an effective way to hamper tumor progression by impairing the paracrine network among tumor, endothelial and polymorphonucleated cells.

Received: January 8, 2015; **Revised:** March 27, 2015; **Accepted:** April 20, 2015

Abbreviations

CN	calcineurin
CIC	calcipressin inhibitor of calcineurin
EGFP	enhanced green fluorescent protein
PMN	plymorphonucleated
NFATc	nuclear factor of activated T cells (cytosolic)
RCAN	regulators of calcineurin proteins
wt	wild-type

Introduction

The protein family of the regulators of calcineurin (RCAN, previously known as DSCR1, MCIP or calcipressin) are conserved from yeast to human and in vertebrates constitute a functional subfamily with three members: RCAN1, RCAN2 and RCAN3 (1,2). These proteins bind to the serine–threonine phosphatase calcineurin (CN) through a conserved calcipressin inhibitor of calcineurin (CIC) motif and when overexpressed, inhibit the activation of the cytosolic Nuclear Factor of Activated T-cells (NFATc) family of transcription factors (3,4). In resting conditions, NFATc (NFATc1-c4) proteins remain highly phosphorylated in the cytosol. Upon an increase in intracellular calcium concentration, CN becomes activated and removes the phosphate groups from NFATc proteins. Dephosphorylation of NFATc unmasks a nuclear localization signal which leads to a rapid translocation into the nucleus where in cooperation with other transcription factors trigger NFATc-dependent gene expression (5).

We have recently shown that an RCAN3 CIC-derived peptide is sufficient to achieve potent inhibition towards NFATc activation in stimulated leukemia T-cells, without affecting the activity of CN towards other substrates (6,7). The mechanism of the CIC motif specificity relies in the presence of a shared PXIXIT sequence responsible for the binding to CN in both RCAN and NFATc. Therefore, RCAN proteins compete with NFATc for the same binding pocket in CN and by these means overexpression of RCAN proteins or the CIC-derived peptide inhibit CN-NFATc signaling (6,8,9).

The NFATc family of transcription factors is involved in the development and function of the immune, cardiovascular, neural, skeletal and muscular systems (10). In the recent years, emerging roles for the NFATc family of transcription factors in tumor progression have been described (11,12). Here, we show that RCAN3 protein and the RCAN3 CIC-derived peptide inhibit the growth of breast cancer cells *in vivo*. Concomitantly, NFATc activity is inhibited in these cells. Our results suggest the inhibition of CN-NFATc pathway in tumor cells as a potential therapeutic target to inhibit tumor progression in breast cancer and highlight a novel key role for human RCAN proteins in the inhibition of tumor progression.

Materials and methods

Cell lines

MDA-MB-231 (ECACC 92020424) and MDA-MB-468 (ATCC-HTB-132) breast cancer cell lines were obtained in 2011, immediately expanded after delivery (up to 6×10^7 cells) and frozen down (1×10^6/vial) such that both cell lines could be restarted after a maximum of 20 passages every 3 months from a frozen vial of the same batch of cells. Control of mycoplasmas was done from a frozen vial. MDA-MB-231 cell line was maintained in Dulbecco's modified Eagle's medium high glucose with glutamax (Invitrogen, Carlsbad, CA) supplemented with 10% fetal bovine serum, 100 U/ml penicillin and 100 µg/ml streptomycin and the MDA-MB-468 cell line was maintained in RPMI 1640 with Glutamax supplemented with 10% fetal bovine serum, 100 U/ml penicillin and 100 µg/ml streptomycin.

Plasmids

The lentiviral backbones pWPI (Addgene #12254) and pWPT (Addgene #12255) were used for this study. The cassettes containing 3× HA tagged RCAN3 (HA-RCAN3, hereafter referred as RCAN3) and EGFP-tagged $R3^{178\text{-}210}$ peptide flanked by *BamHI* sites were inserted into pWPI or pWPT, respectively, after the EF-1α promoter by using Infusion cloning kit (Clontech) following manufacturer's instructions. The RCAN3 AAQ was then subcloned into the pWPI-hemagglutinin (HA-RCAN3 AAQ, hereafter referred as RCAN3 AAQ) backbone using *BamHI* restriction sites. All plasmid constructs were sequenced to verify that no mutations have been created during plasmid construction.

Lentiviral particle production

The lentiviral particles were obtained by transient calcium phosphate transfection of the pWPI and pWPT lentiviral backbones and the psPAX2 and pMD2.g packaging vectors in HEK 293T cells. After 48 h of transfection, the supernatants of the transfected cells were collected, filtered through a 45-µM membrane and ultracentrifuged at 25 000 rpm for 1.5 h in a SW-28 rotor (Beckmann Coulter). Concentrated viruses were collected in cold phosphate-buffered saline, aliquoted and stored frozen at –80°C.

Luciferase reporter gene assay

MDA-MB-231 and MDA-MB-468 cells were seeded at 30% confluence in 48-well plates. After 24 h, the cells were transduced with the lentivirus at 2.5, 5, 10 and 20 multiplicity of infection in 100 µl Dulbecco's modified Eagle's medium 10% fetal bovine serum supplemented with 8 µg/ml polybrene. After overnight incubation with the virus, the medium was replaced and cells were transfected with 400 ng 9×NFAT-luc, 1 ng of pRLNull as an internal transfection control using lipofectamine 2000 (Invitrogen). After 24 h of transfection, cells were stimulated with 1 µM ionomycin, 10 ng/ml phorbol 12-myristate 13-acetate and 10 mM $CaCl_2$. After 8 h of stimulation, cells were analyzed using the Dual-Luciferase Reporter Assay (Promega) following manufacturer's protocol on a multiplate luminometer (Victor X5, Perkin Elmer). Luciferase units were normalized to Renilla luciferase values.

Western blot

MDA-MB-231 cells or tumor xenograft samples were lysed in cold radioimmunoprecipitation assay buffer (50 mM Tris–HCl, 150 mM NaCl, 2 mM ethylene glycol tetraacetic acid, 1% TX-100, 0.25% sodium deoxycholate, 0.1% sodium dodecyl sulfate, 1 mM phenylmethylsulfonyl fluoride) supplemented with protease and phosphatase inhibitor cocktails (Roche, Switzerland). Lysates were then clarified by centrifugation at 16 000×*g* for 10 min at 4°C. The supernatant was then added to 6× Laemmli buffer and incubated for 10 min at 98°C. Protein samples were separated by sodium dodecyl sulfate–polyacrylamide gel electrophoresis and transferred into nitrocellulose membranes. Then, membranes were incubated with anti-cyclooxygenase 2 (COX-2) (Cayman Chemicals, Tallin, Estonia), anti-IL-8 (R & D Systems, MN) anti-EGFP (Clone B2, Santa Cruz, CA), antihemagglutinin (anti-HA) (Clone 12CA5, Roche) and antitubulin (Sigma, St Louis, MI) antibodies. Incubation with secondary horseradish peroxidase-conjugated antibodies allowed signal development by ECL reagent (Millipore, Billerica, MA).

Tumor xenograft experiments

Transduced MDA-MB-231 cells in exponential growth were harvested with trypsin-EDTA (0.05%/0.02%; Invitrogen), washed and examined for viability by trypan blue dye exclusion. Viability was greater than 95%. For primary tumor growth, cells (1×10^6/0.1 ml Dulbecco's modified Eagle's medium high glucose were orthotopically injected into the right fat pad of nude mice. Tumor growth was followed biweekly. At the end of the experiment animals were killed, tumors were surgically removed, weighed and embedded in optimal cutting temperature compound and immediately frozen. Tumor samples (1 mm^3) for RNA and protein analysis were also kept at –80°C until processed.

Immunohistochemistry

Tumor xenograft paraffin sections were blocked with 10% bovine serum albumin for 1 h and then stained with antibodies against NFATc2 (Aviva Systems Biology, San Diego, CA), Ki67 (clone Sp6, Thermo Scientific, MA) and CD31 (BD Biosciences, San Jose, CA) by overnight incubation at 4°C. For NFATc2 staining, sections were washed and incubated with EnVision+System-horseradish peroxidase labeled Polymer Anti-Rabbit antibody (Dako, Denmark). CD31-stained sections were incubated with biotinylated secondary antibodies and avidin–biotin solution (Vectastain ABC Kit) following the instructions. Finally, sections were incubated with 3,3′-Diaminobenzidine (DAB) chromogen (Dako) and counterstained with hematoxylin–eosin, dehydrated and mounted with DPX (Sigma).

Tunel and necrosis assays

Apoptosis quantification was performed by tunel assay using DeadEnd Colorimetric Tunel Assay (G7132, Promega) following manufacturer's procedure. Quantification of apoptotic cells was performed on at least six different high power field (HPF; ×20) per sample.

Tumor slides embedded in paraffin were stained with hematoxylin–eosin. Pictures of entire area tumors were taken with a magnifying glass and necrosis areas were corroborated under the microscopy (60×) before necrosis quantification with ImageJ software. Necrosis quantification was calculated as the necrotic area in percentage within the total area for each tumor. To determine whether significant differences are present between groups, an analysis of variance tests was carried out.

RNA extraction and real-time PCR

RNA from frozen tissue samples (1 mm^3) was extracted using RNAeasy Kit (QIAGEN) following manufacturer's instructions. A total of 2 μg RNA were used to synthesize cDNA using Superscript III (Invitrogen). Quantitative PCR experiments were performed using probes from the Universal probe Library (UPL) (Roche). PCR reactions were carried out in triplicates in a Lightcycler 480 System (Roche). *HPRT1* gene amplification was used as housekeeping control. The sequences for the primers used are listed 5′ to 3′ direction in Supplementary Table 1, available at Carcinogenesis Online.

Results

Ectopic expression of RCAN3 inhibits breast tumor growth *in vivo*

RCAN1 protein has been shown to exert antiangiogenic effects when overexpressed *in vivo*, by blocking the CN-NFATc pathway (13). However, the extent to which this observation applies to the other RCAN family members remains to be addressed. Very recently, high expression of RCAN3 has been shown to be associated with a better overall survival in a cohort of 83 breast cancer patients (14). Therefore, we sought to determine whether RCAN3 inhibits tumor growth in a CN-interaction-dependent manner, using an orthotopic human breast cancer model *in vivo*. To this end, we designed a lentiviral vector to overexpress EGFP and either RCAN3 wild-type (wt) protein or RCAN3 bearing the mutations V197A, V198A and H199Q which disrupt the functional PXIXIT sequence, responsible for the binding to CN, within the conserved CIC motif of RCAN3 (hereafter referred to as RCAN3 AAQ) (Supplementary Figure 1, available at *Carcinogenesis* Online). We then injected 1×10^6 transduced MDA-MB-231 cells overexpressing EGFP and either RCAN3 or RCAN3 AAQ into the mammary fat pad of BALB/c nude mice. The overexpression of RCAN3 protein significantly reduced the growth and weight of the xenografts 5 weeks after injection (Figure 1A and B, respectively). Importantly, RCAN3 AAQ mutant behaved as the control EGFP group, suggesting that the tumor growth inhibitory effects were dependent on the PXIXIT sequence within the conserved CIC motif of RCAN3. The proliferation rate of the tumor cells in the xenograft as determined by human Ki67 protein levels was significantly reduced in the RCAN3-overexpressing tumors (Supplementary Figure 2A, available at *Carcinogenesis* Online and Figure 1C). Moreover, we observed increased apoptosis in the RCAN3-expressing tumors compared to EGFP and RCAN3 AAQ tumors by TUNEL assay (Supplementary Figure 2B, available at *Carcinogenesis* Online and Figure 1D). Altogether, our data show that RCAN3 inhibits MDA-MB-231 breast cancer cells growth *in vivo*.

Ectopic expression of RCAN3 blocks tumor angiogenesis *in vivo*

To characterize tumor angiogenesis, we stained tumor xenograft sections with the endothelial cell marker CD31 antibody. We observed a dramatic reduction of the number of vessels and mean vessel area per HPF in RCAN3-expressing tumors compared to EGFP group (Figure 2A and B, respectively). Remarkably, RCAN3 AAQ expression was unable to inhibit tumor angiogenesis. Moreover, we observed increased, albeit not significant, necrosis in the RCAN3-expressing tumors, suggesting a defective vascularization (Supplementary Figure 2C, available at *Carcinogenesis* Online). Tumor cells are known to stimulate angiogenesis by secreting proangiogenic factors into the tumor microenvironment (15). One of the major tumor proangiogenic factors is vascular endothelial growth factor (16), which accordingly appeared significantly downregulated in RCAN3-expressing tumors, but not in the EGFP or RCAN3 AAQ control groups (Figure 2C). Overall, our results suggest that the overexpression of RCAN3 in breast cancer cells inhibits tumor angiogenesis *in vivo*.

Immune cells, such as neutrophils, promote a proinflammatory environment in the tumor and potentiate angiogenesis and metastasis (17). Interestingly, the presence of polymorphonucleated (PMNs) cells adjacent to the tumor vessels in the xenografts was dramatically reduced in the RCAN3 expressing tumors compared to the RCAN3 AAQ and EGFP control groups, as revealed by quantification of these cells per HPF in hematoxylin–eosin staining sections (Figure 2D and E). The reduction in PMN cells could be due to either a defect on the ability of the RCAN3 expressing tumor cells to recruit immune cells in to the tumor or as a consequence of the reduction in the number of tumor vessels in the tumor.

The cytokines CSF2 and IL-8 have been shown to act as potent chemoattractant factors for the recruitment of polymorphonucleated cells into the tumor microenvironment (18,19). Interestingly, we observed an inhibition of *IL-8* and CSF2 gene expression in the RCAN3 tumors as compared to the EGFP and RCAN3 AAQ control groups (Figure 2F and G, respectively). Furthermore, we found a depletion of the levels of IL-8 protein in the RCAN3 expressing tumors (Figure 2H). IL-8 protein levels were also decreased in the RCAN3 AAQ mutant but to a lower extent than in RCAN3 tumor xenografts, which may be a reflect of the weak interaction of the RCAN3 AAQ with CN that still affects IL-8 production (Supplementary Figure 1, available at *Carcinogenesis* Online). Alternatively, it may be that other protein motifs in RCAN3 are specifically affecting *IL-8* gene expression. As a conclusion, our data suggests that RCAN3 inhibits PMN cell recruitment into the tumor at least in part due to a reduction in the expression of the chemoattractant factors *IL-8* and *CSF2* from the breast cancer cells.

The EGFP-$R3^{178\text{-}210}$ peptide recapitulates the inhibitory effects of RCAN3 on tumor growth

The RCAN3 AAQ mutant does not reproduce the inhibition on tumor angiogenesis, immune cell recruitment and tumor growth observed with the RCAN3 wt protein. These results suggest that the PXIXIT sequence within the conserved CIC motif in RCAN3, responsible for the interaction with CN, is mediating the tumor suppressor effects. We then hypothesized that the overexpression of a peptide spanning the CIC motif of RCAN3 would be sufficient to reproduce the RCAN3-mediated inhibition of tumor growth *in vivo*. Therefore, we designed a lentivirus encoding either EGFP alone or EGFP fused to a short peptide corresponding to the CIC motif of RCAN3 (spanning amino acids 178–210 of human RCAN3, hereafter referred to as EGFP-$R3^{178\text{-}210}$). Then, we injected transduced MDA-MB-231 cells overexpressing the EGFP-$R3^{178\text{-}210}$ peptide or EGFP alone as control into the mammary fat pad of BALB/c nude mice. As shown in Figure 3A and B, the EGFP-$R3^{178\text{-}210}$ peptide was sufficient to reduce tumor growth as compared to the EGFP expressing cells, in the same fashion as the full-length RCAN3

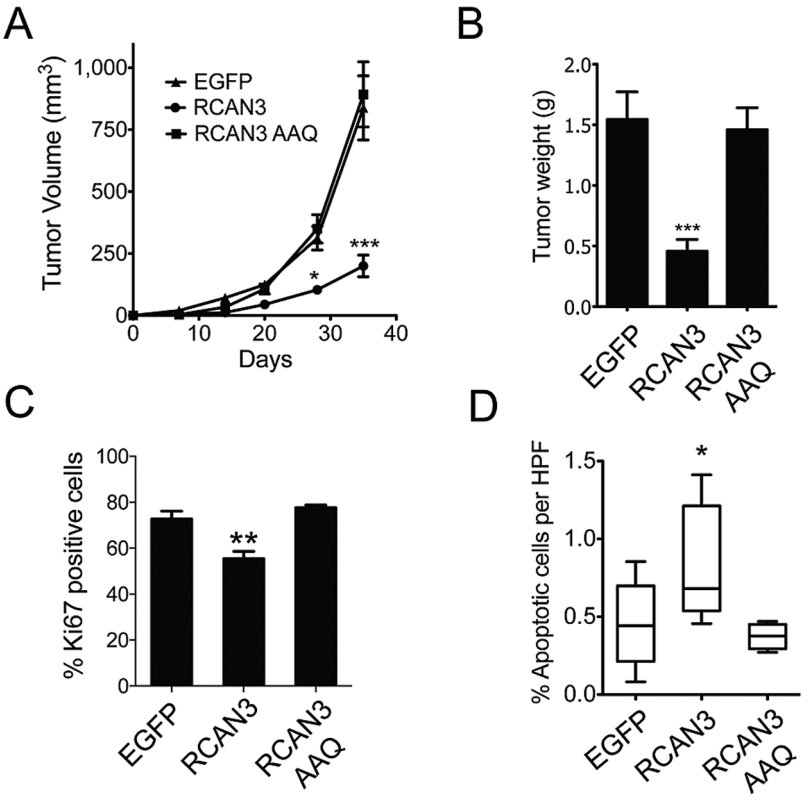

Figure 1. RCAN3 inhibits MDA-MB-231 xenograft growth *in vivo*. (**A**) Tumor xenograft growth curves are represented as mean ± SEM (EGFP $n = 6$, RCAN3 $n = 7$ and RCAN3 AAQ $n = 7$). (**B**) The weights of the tumors of each experimental group are represented as mean ± SEM. (**C**) Data represents the percentage of Ki67 positive nuclei out of the total number of nuclei in tumor xenograft sections (100×) assessed by immunohistochemistry using anti-Ki67 antibody. (**D**) Quantification of the number of apoptotic cells per high power field. EGFP, RCAN3 and RCAN3 AAQ refer to each experimental group tested. Statistical analysis was performed using ANOVA and Bonferroni post-test (*$P < 0.05$; **$P < 0.01$, ***$P < 0.001$).

protein. We also observed reduced levels of Ki67 marker, indicating a lower rate of proliferation of the tumor cells (Supplementary Figure 3A, available at *Carcinogenesis* Online. and Figure 3C) and an increased level of apoptosis as evidenced by TUNEL assay (Supplementary Figure 3B, available at *Carcinogenesis* Online and Figure 3D). In accordance to what we observed in RCAN3 expressing tumors, analysis of tumor vascularization by CD31 staining showed a marked reduction in vessel formation in the EGFP-R3$^{178\text{-}210}$ compared to the EGFP control group (Supplementary Figure 3C, available at *Carcinogenesis* Online and Figure 3E) and we also observed a reduction in the expression of *VEGF* mRNA from the EGFP-R3$^{178\text{-}210}$ xenografts (Figure 3F). As observed in the RCAN3 wt expressing tumors, tumor necrosis in the EGFP-R3$^{178\text{-}210}$ expressing tumors was not significantly increased compared to the EGFP control (Supplementary Figure 3D, available at *Carcinogenesis* Online). Finally, we observed a dramatic reduction in the presence of PMN cells in the EGFP-R3$^{178\text{-}210}$ (Supplementary Figure 3E, available at *Carcinogenesis* Online and Figure 3G). As observed in RCAN3 expressing tumors, expression of *CSF2* and *IL-8* mRNA levels (Supplementary Figure 3F and G, available at *Carcinogenesis* Online) and IL-8 protein levels (Figure 3H) were significantly reduced in the tumors expressing the EGFP-R3$^{178\text{-}210}$ peptide. Therefore, expression of the EGFP-R3$^{178\text{-}210}$ peptide faithfully reproduced the tumor suppressor effects observed for RCAN3 wt protein.

The EGFP-R3$^{178\text{-}210}$ peptide inhibits CN-NFATc signaling in breast cancer cells

We have described a novel tumor suppressor function for EGFP-R3$^{178\text{-}210}$ peptide. This result led us to hypothesize that inhibition of tumor growth is based on the competitive inhibition by the EGFP-R3$^{178\text{-}210}$ peptide towards other PXIXIT-containing proteins for their interaction with CN. In this context, we have previously described that the conserved CIC motif of RCAN proteins inhibits the activation of the CN substrate NFATc in Jurkat T-cells (6,7). Interestingly, inhibition of the CN-NFATc pathway has been shown to play an important role in the phenotype of many different cancer cell types, including breast cancer cell lines (20,21).

To further substantiate this hypothesis, we transduced MDA-MB-231 and MDA-MB-468 cells with a lentiviral vector expressing the EGFP-R3$^{178\text{-}210}$ peptide. A mutated EGFP-R3$^{178\text{-}210}$ peptide (EGFP-R3$^{178\text{-}210}$ peptide bearing the mutations V197A, V198A and H199Q, hereafter referred to as EGFP-R3$^{178\text{-}210}$ AAQ) was included as a control. We observed a dose-dependent inhibitory effect of the EGFP-R3$^{178\text{-}210}$ peptide towards NFATc promoter activation (Figure 4A and B) and nuclear translocation in Ca^{2+} stimulated breast cancer cells (Figure 4C). Accordingly, the mutated EGFP-R3$^{178\text{-}210}$ AAQ peptide was not able to inhibit NFATc translocation or activation. The gene expression of the main NFATc member expressed in MDA-MB-231 and MDA-MB-468 cells, *NFATC2*, was not significantly altered by either EGFP-R3$^{178\text{-}210}$ or the mutated EGFP-R3$^{178\text{-}210}$ AAQ (Figure 4D and E, respectively).

COX-2 (also PTGS2) has been described as an NFATc target gene in MDA-MB-231 cells (22). In accordance, we observed that the EGFP-R3$^{178\text{-}210}$ peptide, and not the mutated EGFP-R3$^{178\text{-}210}$ AAQ, inhibited the induction of COX-2 in a dose-dependent manner in Ca^{2+} stimulated MDA-MB-231 cells (Figure 4F). As a control, incubation of the cells with the CN-NFATc inhibitor

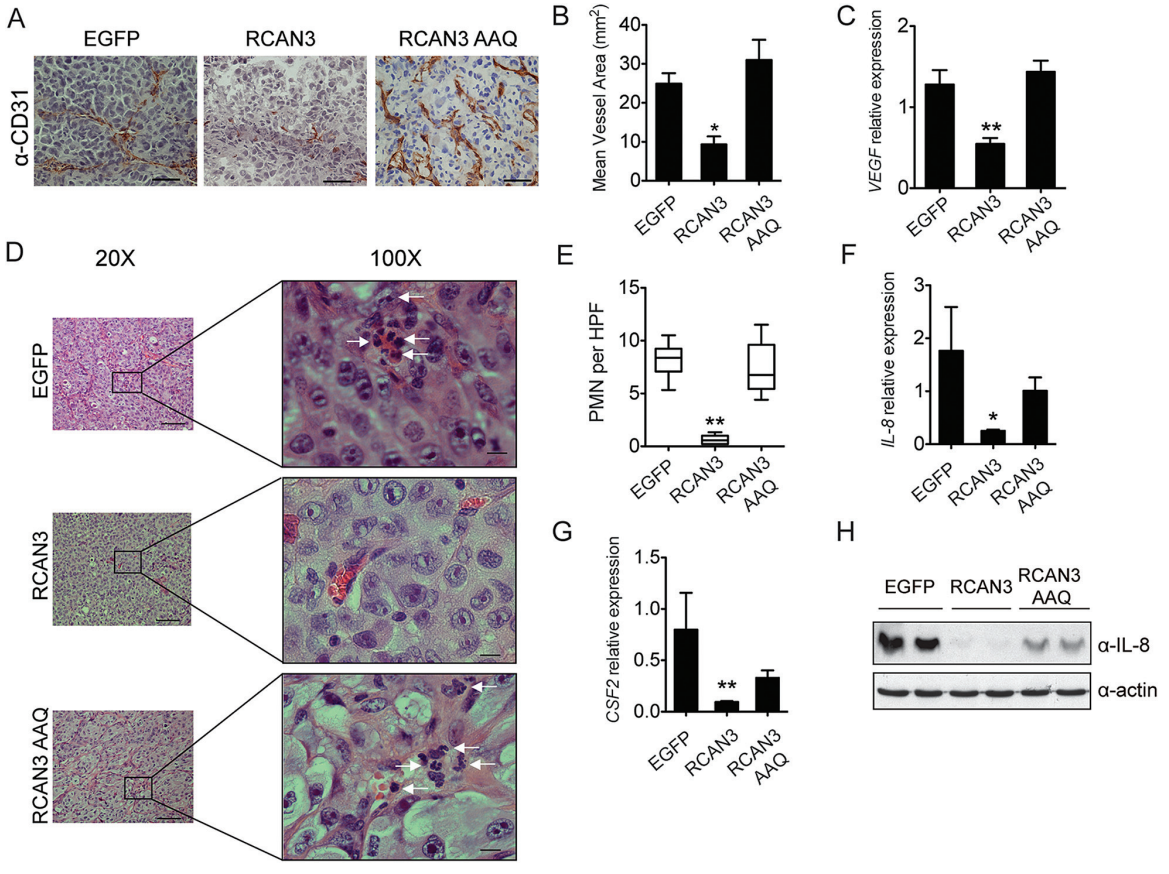

Figure 2. RCAN3 impairs tumor angiogenesis and PMN cell infiltration *in vivo*. (**A**) Representative CD31 staining images of the indicated tumor sections. Scale bars correspond to 100 μm. (**B**) Quantification of mean vessel area in mm² per high power field. Data is presented as mean ± SEM (EGFP $n = 4$; RCAN3 $n = 6$; RCAN3 AAQ $n = 7$). (**C**) Tumor xenograft mRNA levels of human *VEGF* were assessed by quantitative real-time PCR. *HPRT1* gene amplification was used as housekeeping control (EGFP $n = 5$; RCAN3 $n = 7$; RCAN3 AAQ $n = 7$). (**D**) Representative images showing PMN cell tumor infiltration as determined by hematoxylin–eosin staining of the indicated tumor sections. White arrows point out tumor PMN infiltrating cells. Scale bars represent 100 μm (20×) and 20 μm (100×). (**E**) Quantification of the number of PMN cells present per high power field in hematoxylin–eosin-stained slides in each experimental group. The number of PMN cells was counted in at least five different high power field per tumor (EGFP $n = 6$; RCAN3 $n = 7$; RCAN3 AAQ $n = 7$). (**F**, **G**) mRNA levels of *IL-8* (**F**) and CSF2 (**G**) in the tumor xenografts were assessed by real-time qPCR. *HPRT1* gene expression was used as internal control. (**H**) Representative western blot showing the protein levels of IL-8 in tumor protein lysates. Actin is shown as loading control. Data is presented as mean ± SEM. Statistical analysis was performed using ANOVA and Bonferroni post-test (*$P < 0.05$; **$P < 0.01$).

cyclosporine A (CsA) prevented the induction of COX-2 in these cells (Figure 4F, lane 3). Importantly, similar results were obtained when overexpressing RCAN3 wt (Supplementary Figure 4A–E, available at *Carcinogenesis* Online). Thus, the EGFP-R3$^{178\text{-}210}$ peptide inhibits CN-NFATc signaling in human triple negative breast cancer cells.

We then sought to determine whether NFATc2 activation was inhibited in EGFP-R3$^{178\text{-}210}$ expressing MDA-MB-231 cells *in vivo*. Immunohistochemical analysis performed in tumor xenograft sections showed that NFATc2 nuclear staining was markedly reduced in EGFP-R3$^{178\text{-}210}$ expressing tumors compared to the EGFP (Figure 4G). As expected, the tumors expressing RCAN3 wt also presented a predominant NFATc2 cytoplasmic staining, compared to EGFP or RCAN3 AAQ expressing xenografts (Supplementary Figure 4F, available at *Carcinogenesis* Online). Finally, COX-2 protein levels were dramatically reduced in EGFP-R3$^{178\text{-}210}$ expressing tumors when compared to the EGFP control group (Figure 4H). As expected, the same effect was observed in RCAN3 wt expressing tumors (Supplementary Figure 4G, available at *Carcinogenesis* Online). Altogether, these results suggest that the EGFP-R3$^{178\text{-}210}$ peptide inhibits tumor growth *in vivo* at least in part by interfering with the CN-NFATc-COX-2 axis in human breast cancer cells.

Discussion

Our results show that the expression of either RCAN3 or its CIC-derived EGFP-R3$^{178\text{-}210}$ peptide in MDA-MB-231 cells is able to inhibit tumor growth in an orthotopic model of human breast cancer. We describe that the CIC motif of human RCAN3 protein, highly conserved among vertebrate RCANs, has intrinsic tumor suppressor properties *in vivo*. Accordingly, RCAN1 has been previously shown to present antiangiogenic and tumor inhibitory effects (13).

Our data suggests that the tumor suppressor effect of RCAN3 depends on the interaction with CN, as the CN-binding defective RCAN3 AAQ mutant has no effect on tumor growth. Moreover, the EGFP-R3$^{178\text{-}210}$ peptide, which spans the region in RCAN3 responsible for the interaction with CN, is able to reproduce the antitumor properties of the full-length protein. Therefore, we propose that the observed tumor suppressor effects of RCAN3 and EGFP-R3$^{178\text{-}210}$ are explained by a competitive inhibition towards PXIXIT-containing proteins for their interaction with CN. Therefore, the PXIXIT sequence binding site in CN constitutes an important oncogenic signaling node in breast cancer cells.

The NFATc family of transcription factors interacts with CN through a PXIXIT sequence and RCAN proteins are

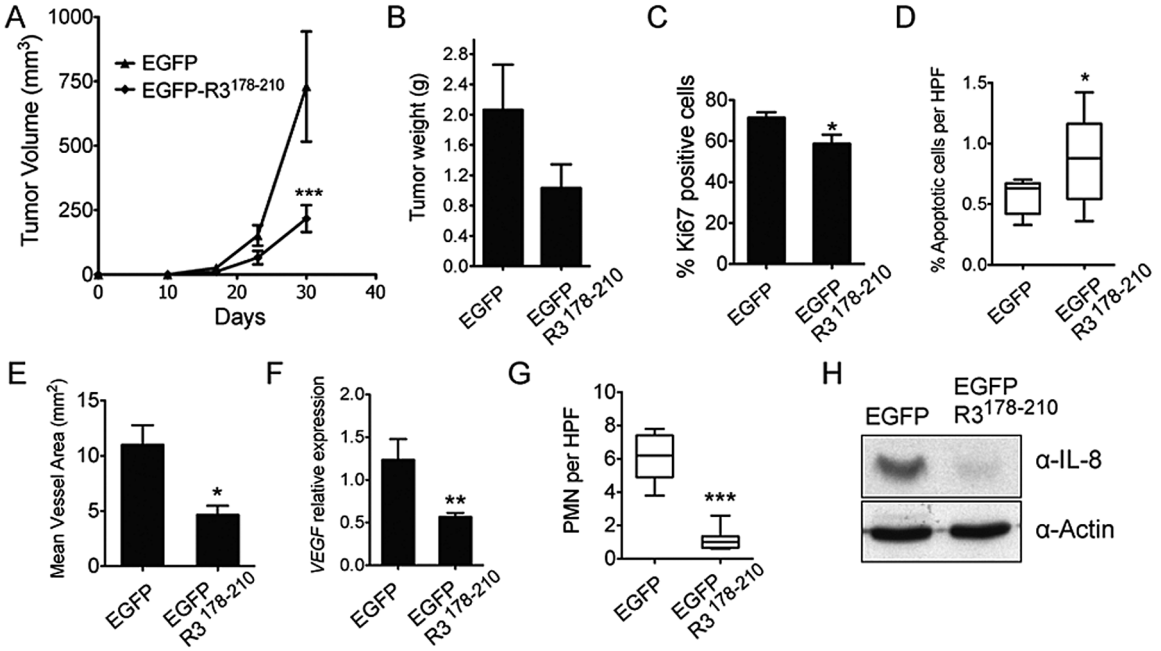

Figure 3. The P-R3$^{178\text{-}210}$ peptide suppresses tumor growth *in vivo*. (**A**) Tumor xenograft growth curves presented as mean ± SEM of MDA-MB-231 cells transduced with lentiviruses encoding EGFP or EGFP-R3$^{178\text{-}210}$ (EGFP n =8 and EGFP-R3$^{178\text{-}210}$ n = 7). (**B**) The weights of the tumors of each experiment are represented as means ± SEM. (**C**) Data represents the percentage of Ki67 positive nuclei out of the total tumor area of tumors overexpressing EGFP and EGFP-R3$^{178\text{-}210}$ tumor samples. Analysis was performed as in Fig. 1C (EGFP n = 7, and EGFP-R3$^{178\text{-}210}$ n = 6). (**D**) Quantification of the number of apoptotic cells per high power field. (**E**) Quantification of mean vessel area in mm^2 per high power field. Data is presented as mean ± SEM (EGFP n = 6; EGFP-R3$^{178\text{-}210}$ n = 7). (**F**) Tumor xenograft mRNA levels of human *VEGF* were assessed by real-time qPCR. *HPRT1* gene was used as internal control (EGFP n = 6; EGFP-R3$^{178\text{-}210}$ n = 8). (**G**) Quantification of the number of PMN cells present per high power field in hematoxylin–eosin-stained slides in each experimental group (EGFP n = 8; EGFP-R3$^{178\text{-}210}$ n = 8). (**H**) Representative western blot showing the protein levels of IL-8 in tumor protein lysates. Actin is shown as loading control. Statistical analysis was performed using *t*-test (*P < 0.05; **P < 0.01, ***P < 0.001).

well-established endogenous modulators of the CN-NFATc pathway (23). NFATc proteins have recently emerged as relevant transcription factors in tumor progression (11,12). Accordingly, in RCAN3 and EGFP-R3$^{178\text{-}210}$ peptide overexpressing tumors, in which tumor growth is impaired, NFATc activation appears inhibited. Furthermore, we observed a dramatic reduction in COX-2 protein levels in RCAN3 and EGFP-R3$^{178\text{-}210}$ peptide overexpressing tumors. COX-2, very frequently highly expressed in tumors, is a well characterized NFATc target gene in different cancer cell lines, including MDA-MB-231 cells (22,24,25). The inhibition of COX-2 enzyme activity has proven to be an effective way to halt tumor progression, as illustrated by the efficacy of nonsteroidal anti-inflammatory drugs and selective COX-2 inhibitors in the prevention and progression of several types of cancers (26,27). Furthermore, it has been shown that inhibition of NFATc proteins activation renders an impaired angiogenic response *in vivo* (28,29). RCAN3 and EGFP-R3$^{178\text{-}210}$ peptide overexpressing xenografts also present a dramatic reduction in tumor angiogenesis, with a concomitant reduction in the gene expression levels of the proangiogenic factors *VEGF* and *IL-8*. In addition, we have found a marked reduction of infiltrating PMN cells in the RCAN3 and EGFP-R3$^{178\text{-}210}$ expressing tumors. The inhibition of the neutrophil chemoattractant and prosurvival factors IL-8 and CSF2 could, at least in part, explain the reduced recruitment of these immune cell types in to the tumor. Of note, the gene expression of both genes has been described to be dependent on NFATc transcription factors, among other cytokines and chemokines (30). Human IL-8 is able to act as a chemoattractant factor for murine neutrophils (31). Also, IL-8 has been shown to be upregulated in breast carcinomas and also in the different compartments of the tumor microenvironment, and low *IL-8* gene expression levels in triple-negative breast cancer have been associated to good patient prognosis, postulating the targeting of IL-8 as an attractive therapy (19,32). As a conclusion, although we cannot rule out the role of other PXIXIT-containing proteins in the phenotype observed, our data suggests that RCAN3 and EGFP-R3$^{178\text{-}210}$ peptide suppress breast cancer growth through competition with NFATc proteins for the binding to CN and, as a consequence, through the inhibition of NFATc activation. Whereas the importance of NFATc in tumor progression has been previously shown in the tumor microenvironment, our data suggest that impaired NFATc activity within the tumor cell hampers the orchestration of a proper angiogenic response from a tumor microenvironment with an unperturbed NFATc function (33).

Breast cancer is a heterogeneous disease encompassing a high variety of entities, of which 15% of newly diagnosed cases are triple-negative breast cancer, characterized by the lack of drug-targetable targets (34). Advancing in this complex disease requires a better knowledge of their molecular profile for the development of specific therapies (35). In our study, we have used the aggressive MDA-MB-231 triple-negative breast cancer cell line in which we observed that the expression of either RCAN3 or the EGFP-R3$^{178\text{-}210}$ peptide produced a significant reduction in the gene expression of *COX-2* and *IL-8*. Therefore, we propose that the development of therapies targeted to the CN-NFATc signaling pathway, based on the RCAN specific modulatory mechanism, which would likely avoid the undesired side effects of the CN inhibitors cyclosporine A and FK506, represent a powerful way to combine the inhibition of the gene expression of the above-mentioned genes implicated in breast cancer progression. The ability of the R3$^{178\text{-}210}$ peptide to inhibit the migration and metastatic potential of breast and

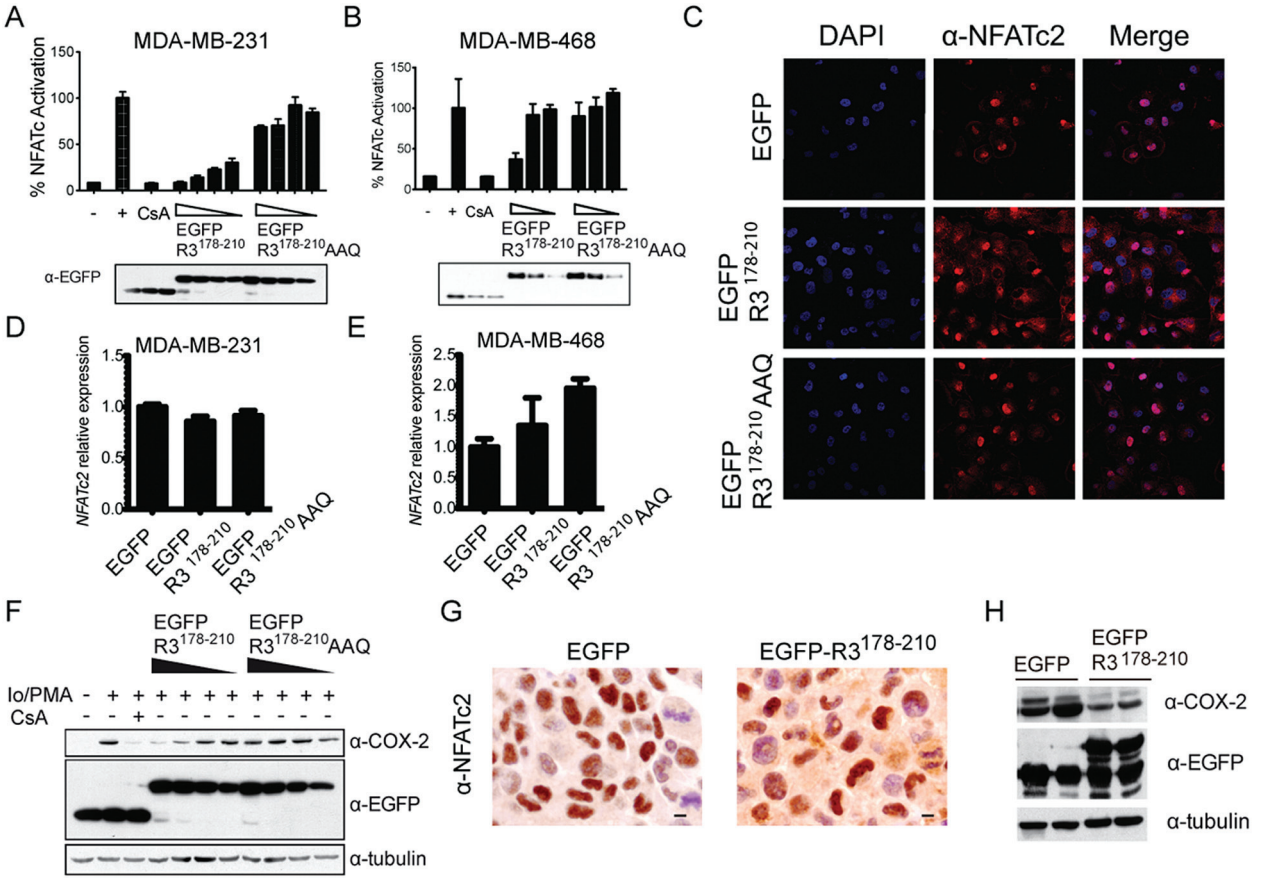

Figure 4. The EGFP-R3$^{178-210}$ inhibits CN-NFATc signaling pathway in human breast cancer cells. (**A**, **B**) NFATc-luciferase reporter gene assay performed in MDA-MB-231 (**A**) and MDA-MB-468 (**B**) breast cancer cells transduced with lentivirus encoding either EGFP-R3$^{178-210}$ or EGFP-R3$^{178-210}$ AAQ at increasing multiplicity of infection and transfected with 9xNFATc-luc and CMV-Renilla reporter plasmids. Luciferase units were normalized to Renilla luciferase values. Data is presented as mean percentage (± SEM) of NFATc activation were the 100% is the activation achieved with Ionomycin/phorbol 12-myristate 13-acetate/$CaCl_2$ alone. Results are representative of at least three independent experiments performed in triplicates. The levels of each protein in each condition was assessed by western blot analysis using anti-EGFP (α-EGFP) antibody. 12-myristate 13-acetate (PMA)/Ca2+; (CsA) stimulated with Io/PMA/Ca2+/cyclosporine A. (**C**) MDA-MB-231 cells transduced with the indicated lentivirus were sorted by EGFP expression and seeded in coverslips and stimulated for 30 min with ionomycin (1 μM) and $CaCl_2$ (10 mM) for 30 min. Then, cells were fixed in 4% PFA and stained with antibodies against NFATc2. Nuclei were counterstained with DAPI. (**D**, **E**) Quantification of *NFATC2* gene expression by real-time qPCR in MDA-MB-231 (**D**) and MDA-MB-468 (**E**) breast cancer cells transduced with lentivirus expressing the indicated constructs. *HPRT1* gene expression was used as housekeeping gene control. The experiments were performed in triplicates and data is presented as mean ± SEM. (**F**) Western blot showing the inhibition of COX-2 induction in stimulated MDA-MB-231 breast cancer cells by EGFP-R3$^{178-210}$ peptide in a dose-dependent manner. The expression of each construct in each condition was assessed using EGFP (α-EGFP) and COX-2 (α-COX-2) antibodies. Tubulin is shown as protein loading control. (**G**) Representative NFATc2 staining images showing reduced NFATc2 nuclear localization in EGFP-R3$^{178-210}$ overexpressing xenografts. Scale bars correspond to 10 μm. (**H**) Representative western blot showing the levels of COX-2, EGFP and EGFP-R3$^{178-210}$ in tumor protein lysates. Tubulin is shown as loading control.

other aggressive cancer types should be addressed in future studies.

Finally, we have previously developed effective screening methods to search for molecules able to displace the CN-RCAN interaction, implying that the identified hits would mimic the NFATc inhibitory effect of the CIC-derived peptide (6,36). Our work provides a strong support to promote the search of compounds sharing the antitumorigenic effects of the R3$^{178-210}$ peptide.

Supplementary material

Supplementary Table 1 and Figures 1–4 can be found at http://carcin.oxfordjournals.org/

Funding

Spanish Ministry of Science and Innovation – MICINN (SAF2009-08216 and BFU2010-22132); Generalitat de Catalunya (2009 SGR1490); IDIBELL PhD fellowship (S.M.-H.).

Acknowledgements

We specially thank Carme Calvis, Agnés Figueras, Nicklas Bassani and Álvaro Aranguren for their technical support and Itziar Martínez-González for her insightful comments on the work.

Conflict of Interest Statement: The authors declare no conflict of interest.

References

1. Davies, K.J. et al. (2007) Renaming the DSCR1/Adapt78 gene family as RCAN: regulators of calcineurin. FASEB J., 21, 3023–3028.
2. Serrano-Candelas, E. et al. (2014) The vertebrate RCAN gene family: novel insights into evolution, structure and regulation. PLoS One, 9, e85539.
3. Aubareda, A. et al. (2006) Functional characterization of the calcipressin 1 motif that suppresses calcineurin-mediated NFAT-dependent cytokine gene expression in human T cells. Cell. Signal., 18, 1430–1438.
4. Mulero, M.C. et al. (2007) RCAN3, a novel calcineurin inhibitor that down-regulates NFAT-dependent cytokine gene expression. Biochim. Biophys. Acta, 1773, 330–341.

5. Crabtree, G.R. et al. (2002) NFAT signaling: choreographing the social lives of cells. Cell, 109 (suppl), S67–S79.
6. Mulero, M.C. et al. (2009) Inhibiting the calcineurin-NFAT (nuclear factor of activated T cells) signaling pathway with a regulator of calcineurin-derived peptide without affecting general calcineurin phosphatase activity. J. Biol. Chem., 284, 9394–9401.
7. Martínez-Høyer, S. et al. (2013) Protein kinase CK2-dependent phosphorylation of the human Regulators of Calcineurin reveals a novel mechanism regulating the calcineurin-NFATc signaling pathway. Biochim. Biophys. Acta, 1833, 2311–2321.
8. Martínez-Martínez, S. et al. (2009) The RCAN carboxyl end mediates calcineurin docking-dependent inhibition via a site that dictates binding to substrates and regulators. Proc. Natl. Acad. Sci. USA, 106, 6117–6122.
9. Mehta, S. et al. (2009) Domain architecture of the regulators of calcineurin (RCANs) and identification of a divergent RCAN in yeast. Mol. Cell. Biol., 29, 2777–2793.
10. Wu, H. et al. (2007) NFAT signaling and the invention of vertebrates. Trends Cell Biol., 17, 251–260.
11. Müller, M.R. et al. (2010) NFAT, immunity and cancer: a transcription factor comes of age. Nat. Rev. Immunol., 10, 645–656.
12. Mancini, M. et al. (2009) NFAT proteins: emerging roles in cancer progression. Nat. Rev. Cancer, 9, 810–820.
13. Baek, K.H. et al. (2009) Down's syndrome suppression of tumour growth and the role of the calcineurin inhibitor DSCR1. Nature, 459, 1126–1130.
14. Huang, C.C. et al. (2013) Concurrent gene signatures for han chinese breast cancers. PLoS One, 8, e76421.
15. Hanahan, D. et al. (2011) Hallmarks of cancer: the next generation. Cell, 144, 646–674.
16. Nagy, J.A. et al. (2007) VEGF-A and the induction of pathological angiogenesis. Annu. Rev. Pathol., 2, 251–275.
17. Hanahan, D. et al. (2012) Accessories to the crime: functions of cells recruited to the tumor microenvironment. Cancer Cell, 21, 309–322.
18. Gomez-Cambronero, J. et al. (2003) Granulocyte-macrophage colony-stimulating factor is a chemoattractant cytokine for human neutrophils: involvement of the ribosomal p70 S6 kinase signaling pathway. J. Immunol., 171, 6846–6855.
19. Waugh, D.J. et al. (2008) The interleukin-8 pathway in cancer. Clin. Cancer Res., 14, 6735–6741.
20. Jauliac, S. et al. (2002) The role of NFAT transcription factors in integrin-mediated carcinoma invasion. Nat. Cell Biol., 4, 540–544.
21. Yoeli-Lerner, M. et al. (2005) Akt blocks breast cancer cell motility and invasion through the transcription factor NFAT. Mol. Cell, 20, 539–550.
22. Yiu, G.K. et al. (2006) NFAT induces breast cancer cell invasion by promoting the induction of cyclooxygenase-2. J. Biol. Chem., 281, 12210–12217.
23. Li, H. et al. (2011) Interaction of calcineurin with substrates and targeting proteins. Trends Cell Biol., 21, 91–103.
24. Duque, J. et al. (2005) Expression and function of the nuclear factor of activated T cells in colon carcinoma cells: involvement in the regulation of cyclooxygenase-2. J. Biol. Chem., 280, 8686–8693.
25. Iñiguez, M.A. et al. (2000) An essential role of the nuclear factor of activated T cells in the regulation of the expression of the cyclooxygenase-2 gene in human T lymphocytes. J. Biol. Chem., 275, 23627–23635.
26. DuBois, R. et al. (2003) The emerging role and potential of COX-2 inhibitors. Clin. Adv. Hematol. Oncol., 1, 97–98.
27. Iñiguez, M.A. et al. (2003) Cyclooxygenase-2: a therapeutic target in angiogenesis. Trends Mol. Med., 9, 73–78.
28. Hernández, G.L. et al. (2001) Selective inhibition of vascular endothelial growth factor-mediated angiogenesis by cyclosporin A: roles of the nuclear factor of activated T cells and cyclooxygenase 2. J. Exp. Med., 193, 607–620.
29. Urso, K. et al. (2011) NFATc3 regulates the transcription of genes involved in T-cell activation and angiogenesis. Blood, 118, 795–803.
30. Rao, A. et al. (1997) Transcription factors of the NFAT family: regulation and function. Annu. Rev. Immunol., 15, 707–747.
31. Asfaha, S. et al. (2013) Mice that express human interleukin-8 have increased mobilization of immature myeloid cells, which exacerbates inflammation and accelerates colon carcinogenesis. Gastroenterology, 144, 155–166.
32. Rody, A. et al. (2011) A clinically relevant gene signature in triple negative and basal-like breast cancer. Breast Cancer Res., 13, R97.
33. Tripathi,P. et al. (2014) Activation of NFAT signaling establishes a tumorigenic microenvironment through cell autonomous and non-cell autonomous mechanisms. Oncogene, 33, 1840–1849.
34. Hudis, C.A. et al. (2011) Triple-negative breast cancer: an unmet medical need. Oncologist, 16 (suppl. 1), 1–11.
35. Crown, J. et al. (2012) Emerging targeted therapies in triple-negative breast cancer. Ann. Oncol., 23 (suppl. 6), vi56–vi65.
36. Carme Mulero, M. et al. (2010) A fluorescent polarization-based assay for the identification of disruptors of the RCAN1-calcineurin A protein complex. Anal. Biochem., 398, 99–103.